

## HIGH GRADIENT TESTS OF THE HINS SSR1 SINGLE SPOKE RESONATOR

I. Gonin, T. Khabibouline, G. Lanfranco, A. Mukherjee, J. Ozelis, L. Ristori, D. A. Sergatskov, R. Wagner, R. Webber, FNAL, Batavia, IL 60510, U.S.A.

### Abstract

Eighteen  $\beta = 0.21$  superconducting single spoke resonators comprise the first stage in the cold section of the 8-GeV H Linac for Fermilab's proposed Project X. After Buffered Chemical Polishing and High Pressure Rinse, one resonator has undergone high gradient RF testing at 2.0 – 4.5 K in the Vertical Test Stand at Fermilab. We present measurements of the surface resistance as a function of temperature and the quality factor as a function of accelerating field. The resonator reached an accelerating field of 18.0 MV/m.

### SUPERCONDUCTING SPOKE RESONATORS IN PROJECT X AND HINS

The High Intensity Neutrino Source (HINS) program at Fermilab will demonstrate new technologies suitable for the low-energy front-end of a high intensity, 8-GeV, H Linac based on independently phased superconducting resonators [1]. The pulsed Linac (9 mA x 1 msec x 5 Hz) is the key new component of Fermilab's proposed Project X.

Three superconducting spoke resonators comprise the low energy portion of the Linac's cold section and operate at 325 MHz, one quarter of the frequency of the ILC type cavities that make up the high energy end. Two Single Spoke Resonators, SSR1 with  $\beta_g = 0.21$  [2] and SSR2 with  $\beta_g = 0.4$ , will be built and operated as part of HINS.

Two SSR1 prototypes, SSR1-01 at Zanon [3] and SSR1-02 at Roark [4], have been fabricated. Figure 1, an exploded-view schematic of SSR1, shows the main features. The spoke spans the inner diameter of the shell, and two accelerating gaps are formed between the spoke and the endwalls. Liquid helium flows around the outer surfaces of the shell and endwalls and through the spoke.

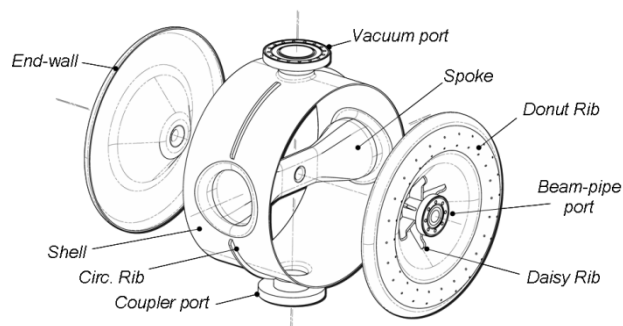


Fig. 1: Exploded-view schematic of SSR1.

The cavity operates at a temperature  $T = 4.4$  K, a nominal accelerating gradient  $E_{acc} = 10$  MV/m, and an intrinsic quality factor  $Q_0 > 0.5 \times 10^9$  at the accelerating gradient.

After the first prototype, SSR1-01, arrived at Fermilab from Zanon, low gradient RF measurements, including bead pulls, were made to check the resonant frequency and compare the field profile with the calculation of Microwave Studio (MWS) [5]. The agreement was very good, with a field flatness of 99.7%.

### BUFFERED CHEMICAL POLISHING AND HIGH PRESSURE RINSE

The interior surface of SSR1-01 was then prepared for testing at high gradient. The cavity was immersed in a bath of Ultra-Pure Water (UPW) with a degreasing agent and ultrasonically cleaned. It was then taken to the ANL G150 facility for Buffered Chemical Polishing (BCP), followed by a High Pressure Rinse (HPR).

The BCP used the standard  $\text{HF}:\text{HNO}_3:\text{H}_3\text{PO}_4(1:1:2)$  acid mixture. During BCP, acid flow and temperature were controlled in the following manner. The cavity was immersed in a bath of UPW that was initially cooled to 7.5 °C by a continuously operating chiller. The cavity interior, sealed from the water bath, was connected to a pump for acid circulation. The cavity was oriented with the power coupler port and the vacuum port along the vertical axis and the beam pipes along the horizontal axis. In order to begin etching, acid (earlier chilled to 14 °C) was pumped up through the bottom port to fill the interior of the cavity plus an "overflow bucket" connected to the top port. After shutting off the source of acid, the closed loop circulation pump drew acid from the overflow bucket and sent it back to the cavity through flanges on both beam pipes. Heat generated by the etching was dissipated through the cavity walls (including the spoke walls) to the continuously cooled water bath.

In order to obtain a total etching of  $\sim 120$   $\mu\text{m}$  and keep the niobium content in the acid below 10 g/l, spent acid was replaced with fresh acid about half way through the etching. Given the asymmetry in the acid flow pattern, the cavity was flipped top to bottom between the two etching sessions. The reduction in wall thickness was monitored at 20 locations using an ultrasonic thickness gauge.

The wall thickness reduction averaged 119  $\mu\text{m}$  after a total etching time of 160 minutes. The acid temperature averaged 15.9 °C and ranged between 14.9 °C and 17.0 °C during the etching. The thickness reduction was not as uniform as hoped, and we have plans to distribute the acid flow more uniformly in the future.

After BCP, the SSR1-01 was moved to the G150 class 10 clean area for HPR. The UPW distribution consists of a long wand with a nozzle at the end that produces six

water jets, two each at  $+45^\circ$ ,  $90^\circ$ , and  $-45^\circ$  to the wand axis. The wand rapidly rotates about the axis and travels along the axis (into or out of the cavity) at  $\sim 3$  cm/min. After completing the HPR (20 minutes at each of 6 orientations), the cavity was left in a good orientation for drainage and left to dry in the class 10 clean area overnight.

## HIGH GRADIENT MEASUREMENTS

The Fermilab Vertical Test Stand (VTS), a liquid helium dewar designed for high-gradient testing of bare 9-cell ILC cavities, was used for the first cold test of the bare SSR1-01. The SSR1-01 was mounted in the VTS dewar with the power coupler port up and the beam pipe along the horizontal axis.

There have been three test sessions in the VTS; Test 1 in February, 2008, Test 2 in March, 2008 and Test 3 in July, 2008. For Test 1 (the first cold test of the cavity) and Test 2, the VTS did not yet have a cavity vacuum system, so the SSR1 was evacuated (to  $2 \times 10^{-6}$  Torr for Test 1) and sealed before installation into the dewar.

In Test 1,  $Q_0$  was measured as a function of temperature,  $T$ , as the temperature was lowered from 4 K to 2 K at  $E_{acc} = 2$  MV/m. As shown in Figure 2, this data was used to obtain the surface resistance,  $R_s(T) = R_0 + R_{BCS}(T)$  with a fit residual resistance of  $R_0 = 5.1$  n $\Omega$ .

In Test 1, the resonant frequency was measured as a function of the liquid helium bath pressure, as shown in Figure 3. The measured pressure sensitivity agrees quite well with the value of  $-630$  Hz/Torr predicted by the MWS simulation of the bare cavity (the simulation predicts a much smaller value of  $-30$  Hz/Torr when the helium vessel is attached).

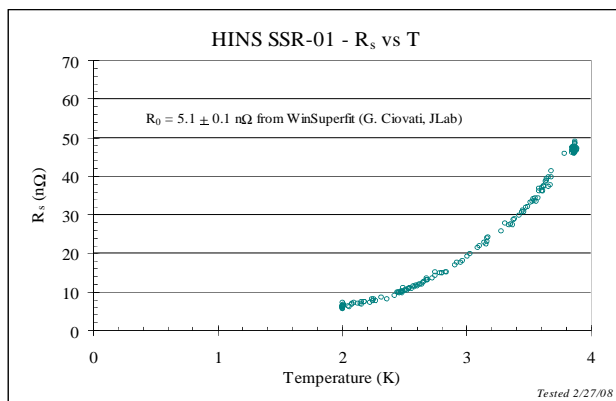


**Fig. 2:** The measured variation of surface resistance with temperature.

In Test 2, the resonant frequency was measured as a function of  $E_{acc}^2$ , as shown in Figure 4. The measured Lorentz force detuning coefficient of approximately  $-4$  Hz/(MV/m) $^2$  agrees much better with the simulation's prediction of the cavity with the helium vessel attached,  $-3.8$  Hz/(MV/m) $^2$ , than bare,  $-13.4$  Hz/(MV/m) $^2$ . This is not yet understood.

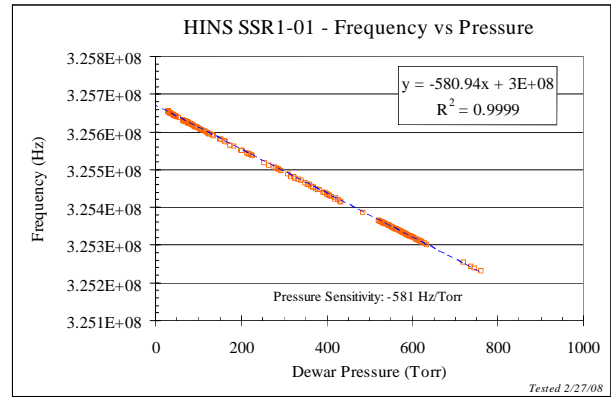


**Fig. 3:** The measured variation of resonant frequency with liquid helium pressure.

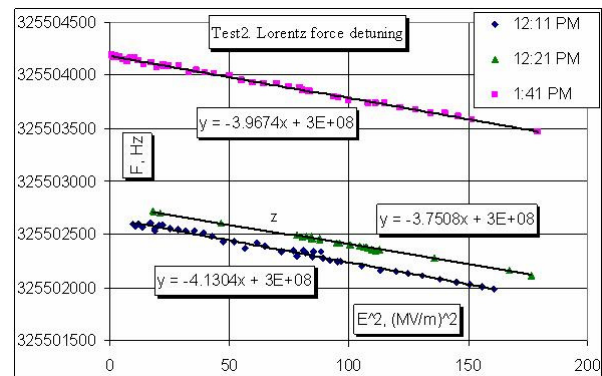


**Fig. 4:** The measured variation of resonant frequency with  $E_{acc}^2$ . Change in dewar pressure accounts for the frequency shift with time.

## $Q_0$ .vs. $E_{acc}$ scans

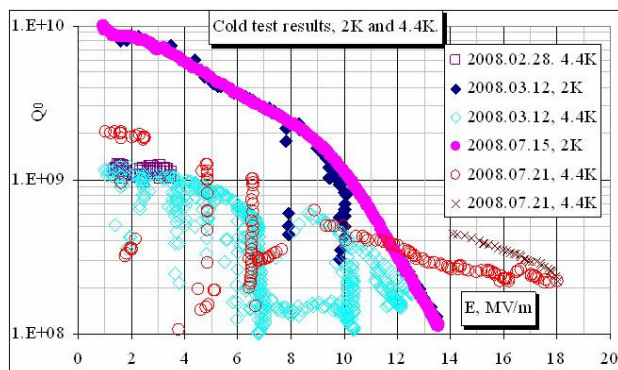
When increasing  $E_{acc}$  at 2 K in Test 1, several multipacting barriers were encountered and we could not process beyond one near 6 MV/m. During Test 1, the SSR1-01 was instrumented with temperature monitors on the shell, around most of the circumference at the endwalls and around the ends of the spoke. The monitors indicated that the multipacting occurred only at the bottom of the cavity near the vacuum port.

After ending Test 1 and warming to room temperature, the cavity pressure was measured to be 1 to 2 orders of magnitude higher than expected if the cavity was just sitting on the shelf. A Residual Gas Analysis (RGA) indicated that the cavity contained water and hydrogen, but no detectable helium. The poor vacuum and evidence for multipacting predominately on the bottom indicated a possible problem with condensates forming during both the cool down and the multipacting.

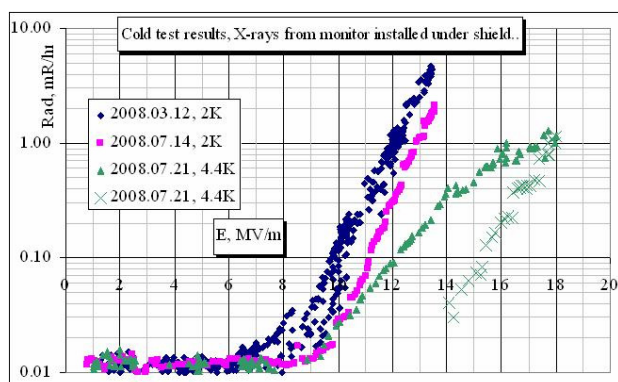
Test 2 began with a better warm cavity vacuum of  $1.2 \times 10^{-7}$  Torr. The  $E_{acc}$  scan of  $Q_0$  at 2 K, shown in Figure 5, reached 13.5 MV/m before field emission prevented further increase with our 200 W power supply. The multipacting barriers shown in the figure were also encountered upon subsequent  $E_{acc}$  scans in Test 2.

Figure 6 shows the X-ray intensity from a detector installed just above the VTS dewar's top plate. Field

emission clearly became a significant power drain above  $\sim 8$  MV/m in Test 2. An  $E_{\text{acc}}$  scan of  $Q_0$  at 4.4 K, shown in Figure 5, ended with a thermal quench at 12.5 MV/m.



**Fig. 5:**  $Q_0$  versus  $E_{\text{acc}}$  scans at 2 K and 4.4 K from the three tests. Test 1: 2008.02, Test 2: 2008.03, and Test 3: 2008.07. Data from the reverse scan at 4.4 K in Test 3 are indicated by X's.



**Fig. 6:** X-rays detected during the  $Q_0$  versus  $E_{\text{acc}}$  scans at 2 K and 4.4 K. Test 2: 2008.03, and Test 3: 2008.07. Data from the reverse scan at 4.4 K in Test 3 are indicated by X's.

With the presence of field emission at high  $E_{\text{acc}}$ , we hoped to do an improved HPR before the next VTS test, but the VTS scheduling allowed for a third test before another HPR could be arranged at ANL. Steps were taken to optimize the cavity vacuum throughout Test 3. A two day long 120 °C vacuum bake was performed shortly before the cavity was installed in the VTS. In addition, the newly commissioned cavity vacuum system of the VTS allowed a vacuum at the cavity of  $\sim 8 \times 10^{-8}$  Torr.

Test 3 started with an  $E_{\text{acc}}$  scan of  $Q_0$  at 2 K, and the result, shown in Figure 5, was essentially identical to that from Test 2, with the important exception that after the initial scan, the cavity no longer fell into multipacting barriers near the operating gradient of 10 MV/m when raising the field. The VTS was left to warm to approximately 3.5 K overnight, and the following morning  $E_{\text{acc}}$  could not be raised above 15 kV/m, indicating a helium leak. After warming up to room temperature, helium was clearly seen in an RGA, but efforts to isolate the source of the leak at that time were unsuccessful.

**High-Intensity Linacs & Rings: New Facilities and Concepts**

After cooling back down to 4.4 K, the field could again be raised, and the  $E_{\text{acc}}$  scan of  $Q_0$  shown in Figure 5 was taken. In this case, data taken during the initial increase in field (including processing multipacting barriers) and data subsequently taken working backward from the maximum field are plotted with different symbols. There are several interesting features of this scan.  $Q_0$  at low  $E_{\text{acc}}$  is nearly a factor of two higher than that recorded in the 4.4 K scans in Tests 1 and 2. This corresponds to a reduction in surface resistance from 70 n $\Omega$  to 45 n $\Omega$ , and this may be due to the 120 °C bake. Note that an improvement was observed in  $R_s(4.4\text{K})$ , but not in  $R_s(2\text{K}) \cong R_0$ .

Up to 10 MV/m, the cavity behaved similarly to Test 2, but after 10 MV/m, the cavity properties started changing. The intensity of X-rays dropped (Figure 6) and  $Q_0$  increased (Figure 5). It appears that helium processing of field emitters had occurred, allowing  $E_{\text{acc}}$  to reach 18 MV/m, well beyond the earlier maxima of 12.5 MV/m at 4.4 K and 13.6 MV/m at 2 K. This scan could have continued to higher field levels, since power was not yet limited by field emission.

A backward scan in field was started to record any change in  $Q_0$  after the initial processing. As evidenced by the reduced X-ray intensity (Figure 6), field emission was considerably lower in the backward scan with a corresponding increase in  $Q_0$  (Figure 5). After recording the data point at 14 MV/m, the cavity again became inoperable, indicating further problems with the helium leak. Test 3 ended, and the leak was eventually isolated to the RF feed through for the power coupler antenna. The helium leak was probably a two-edged sword, sometimes not allowing operation (possibly due to increased multipacting), but also allowing the processing of field emitters to achieve higher fields.

## ACKNOWLEDGEMENTS

The authors wish to acknowledge the efforts of S. Gerbick, M. Kedzie, and M. Kelly of ANL; T. Arkan, D. Arnold, D. Assell, G. Romanov, J. Williams and B. Smith of Fermilab; and T. Roark and D. Osha of Roark.

## REFERENCES

- [1] P.N. Ostroumov et al, "Front End Design of a Multi-GeV H-Minus Linac", Proc. Of the PAC-2005, Knoxville, Tennessee, May 2005.
- [2] G. Lanfranco et al., "Production of 325 MHz single spoke resonators at FNAL", Proc. of PAC07, Albuquerque, New Mexico, USA.
- [3] Ettore Zanon Spa – Via Vicenza 113 – 36015 Schio (Vi) Italy – www.zanon.com.
- [4] C.F. Roark Welding & Engineering Co, Inc. – 136 N. Green St. – Brownsburg, IN 46112, USA – www.roarkfab.com.
- [5] CST MICROWAVE STUDIO® (CST MWS), www.cst.com.